JRIFST
Original Paper

www.journals.rifst.ac.ir
Journal of Research and Innovation
in Food Science and Technology

DOI: 10.22101/jrifst.2022.318480.1303

Analyzing the Effects of Agar gum on the Textural and Rheological Properties of Cold-set whey Protein Isolate Emulsion-filled Gel

Mohammad Reza Salahi [1], Seyed Mohammad Ali Razavi [2*], Mohebbat Mohebbi [2]

1- PhD student, Department of Food Science and Technology, Ferdowsi University of Mashhad (FUM), Mashhad, Iran
2- Professor, Department of Food Science and Technology, Ferdowsi University of Mashhad (FUM), Mashhad, Iran
*Corresponding author (s.razavi@um.ac.ir)

Abstract

This study evaluated the impact of agar gum (AG) (0-0.7% w/w) on the textural, rheological, and held water characteristics of cold-set whey protein isolate emulsion filled gel (EFG). Steady shear results showed that EFGs had a shear-thinning flow behavior, and with increasing AG concentration, the consistency coefficient increased from 339.12 $Pa.s^n$ (no AG) to 951.46 $Pa.s^n$ (0.7% AG). The amplitude sweep assay illustrated that the AG level had a meaningful effect on the rheological parameters so that G'_{LVE}, G''_{LVE}, G_f and τ_F increased, and $\mathrm{Tan}\,\delta_{LVE}$ decreased with an increase in the AG level. Based on the frequency sweep test, adding AG significantly enhanced the magnitudes of k' and k'', so that their values increased from 5311.8 and 939.9 Pa in the control to 25080.6 and 3574.9 Pa in the 0.7% AG-contained sample, respectively. Also, the parameters of the strength of the network (5380.1-25344.3 $Pa.s^{1/z}$), the network extension (10.05-15.59) and the extent of departure from the *Cox-Merz* rule (3476.80 to 21509.44 Pa) increased directly as a result of the rise in AG content. In the composite EFG with 0.7% AG, the highest initial tangent modulus and fracture stress were recorded, which showed lower fracture strain and equal fracture energy in comparison to the control sample. Research results also showed that the held water decreased meaningfully at a high concentration of AG. These results add to the knowledge of the protein-polysaccharide interactions that can be helpful in the production of new functional foods.

Received: 2021.12.06
Accepted: 2022.01.30

Keywords
Agar
Cold set emulsion-filled gel
Fracture properties
Rheology
Whey protein

Introduction

The emulsion-filled gel (EFG) is an important class of food products ranging from semisolid to solid in which oil droplets are entrapped as filler particles in the gel matrix (Farjami & Madadlou, 2019). In these systems, the benefits of emulsions are combined with the physical and mechanical qualities of gels, for instance, delivering different kinds of lipid-soluble and water-soluble functional substances (such as probiotics, drugs, phenolic compounds, vitamins, minerals, carotenoids, and flavors) within a single formulation with a long shelf life is a key advantage of EFGs (Pandey *et al*., 2016;

Lu, Mao, Hou, Miao, & Gao, 2019; Torres, Murray, & Sarkar, 2016). It is possible to design systems with desired textural and rheological properties to control the delivery of incorporated ingredients in polysaccharides, which are the underpinnings of product quality and authenticity. As a consequence, to develop novel and attractive food products, the interactions between proteins and polysaccharides are garnering a lot of attention in the food sector (Xiong *et al*., 2017). Protein-polysaccharide interactions can be either attractive or repulsive, resulting in complexes or thermodynamic incompatibilities which depend on the biopolymer characteristics and environmental factors (Çakır & Foegeding, 2011).

Many research organizations have relied on whey proteins in the past and continue to do so now because whey proteins have appealing functional properties and high nutritional value and are used in a variety of food systems (Behrouzain, Razavi, & Joyner, 2020). Forming three-dimensional solid-like networks through the aggregation and cross-linking of protein molecules is one of the most important functional characteristics of whey proteins.

Polysaccharides that can form self-supporting gels can be used to manipulate the technological and functional properties of protein-based gels. Agar forms thermo-reversible gels, which gelation is induced by cooling of the heated sample. Agar is a sulfated biopolymer that is found in the cell walls of agrophyte algae and comprises two major components: agarose and agaropectin. When agar solution is cooled, its molecules change from linear to double helix, and with the increase of hydrogen bonds, a stable three-dimensional network structure is formed. With the temperature reduced further, the double helices aggregate to form a hard gel (Zhang *et al*., 2020).

The common food processing procedures are heat-set and cold-set methods, which transform globular EFGs by manipulating gelling polymers, portions of the oil/water phase, the size of the oil droplets, and the gelation method.

The major biopolymers utilized to make gel structures are proteins and protein-based oil-in-water emulsions into soft to solid-like forms. During the heat treatment in the heat-set process, three separate stages, namely denaturation, aggregation, and gelation, occur simultaneously. But in the cold-set process, denaturation and aggregation phases are separate from the gelation phase (Alavi, Momen, Emam-Djomeh, Salami, & Moosavi-Movahedi, 2018; Vilela, Cavallieri, & Da Cunha, 2011). In contrast to heat-set methods, which are not ideal for delivering heat-sensitive compounds, cold-set methods create gels that are acceptable for delivering heat-sensitive substances, allowing their usage in food formulations to be increased.

Many studies have indicated that using polysaccharides to improve gelling properties of proteins in the heat-set method has proven successful (Yang, Wang, Li-Sha, & Chen, 2021; (Chaux-Gutiérrez, Pérez-Monterroza, & Mauro, 2019; Zheng, Beamer, Matak, & Jaczynski, 2019; Zhao, Chen, Hemar, & Cui, 2020; Sow, Tan, & Yang, 2019; Li *et al*., 2020). On the opposite side, only a small number of studies have looked at how polysaccharides affect cold-set protein emulsion gel systems (Khalesi, Emadzadeh, Kadkhodaee, & Fang, 2019; Mao, Miao, Yuan, & Gao, 2018). To the knowledge of the authors, WPI-AG mixed EFG systems produced by the cold-set method have not yet been studied. Therefore, the current research aimed to characterize the effect of AG on whey protein emulsion-filled gels based on the steady and dynamic rheological, textural, and held water characteristics.

Materials and Methods

Materials

Whey protein isolate (WPI) containing 98.9% protein (dry basis), 0.3 wt% fat, 1.7

wt% ash, and 4.6 wt% moisture was gifted by Agropur Ingredients Co. (Le Sueur, Minnesota, USA). Sunflower oil was purchased from a local food store and used right away without further purification. Agar gum (Product # W201201) and calcium chloride dihydrate ($CaCl_2.2H_2O$) (molecular weight: 147.01 gr/mol) were bought from Sigma Aldrich Co. (USA) and Merck Co. (Darmstadt, Germany), respectively. Also, to create all of the dispersions, deionized water was used.

Samples preparation

Preparation of the WPI emulsion

WPI (1% w/w) was dispersed in deionized water and gently stirred with a magnetic stirrer (300 rpm, 2 h) to completely hydrate the proteins. To achieve a final content of 20% w/w oil, an adequate amount of sunflower oil was added to the WPI dispersion and the sample was stirred for 1 h. The premix was then homogenized using a laboratory rotor-stator homogenizer (model IKA, Germany) at a speed of 15000 rpm for 3 min at room temperature. Subsequently, emulsification of the coarse emulsions was performed by an ultrasonic homogenizer (model UHP-400, 20 kHz, Ultrasonic Technology Development Co., Iran) for 5 min equipped with a cylindrical titanium probe (13 mm in diameter) which was immersed 2.0 cm below the surface of the pre-emulsions. Using a cold-water bath, the temperature was maintained at 25-30 ℃ during the sonication process. The remaining WPI was gently added to the emulsion to obtain a final concentration of 5.5% w/w to form self-supporting structures, and the sample was stirred with a magnetic stirrer (4 h, 300 rpm). The samples were then subjected to ultrasound for another one minute to ensure uniform emulsion preparation.

Preparation of emulsion filled gels

The stock dispersions of AG were made by dispersing sufficient quantities of AG powder in deionized water. The prepared emulsions and AG dispersions were put in Schott bottles and heated at 90℃ for 40 min in a water bath, and subsequently heated on a magnetic stirrer plate and kept at boiling temperature for 3 min until the agar was completely dissolved. Immediately after heating, WPI emulsion and AG dispersion were mixed at a ratio of 3:1 into a cylindrical container with a diameter of 55 mm on a stirring plate at a speed of 600 rpm for 6-8 min to obtain a homogeneous mixture. After decreasing the temperature to 60℃ for the ion-induced gelation, the mixtures were charged with an appropriate volume of $CaCl_2$ stock solution to a final concentration of 10 mM of salt and homogenized with a stirrer (600 rpm for 2 min). To stabilize the EFG network, prepared samples were immediately incubated at 4℃ for 20-22 h. The final mixed EFG samples contained varying amounts of AG (0, 0.1, 0.3, 0.5, and 0.7% w/w) as well as constant protein and sunflower oil concentrations of 5.5% w/w and 20% w/w, respectively.

Rheological measurements

A Physica MCR 301 rheometer (Anton Paar, GmbH, Graz, Austria) equipped with a parallel-plate geometry was used to assess the rheological parameters of the EFG samples with a diameter of 50 mm and a gap size of 2 mm. Using a Peltier system (Viscotherm VT2, Phar Physica), the temperature was held at 20℃ (±0.01 ℃) throughout the tests. The perimeters of EFGs were coated with silicone oil to avoid water loss. At least two duplicates of each rheological measurement were performed.

Steady shear test

The steady flow characteristics of EFGs were investigated at a shear rate range of 0.01-10 s^{-1} and 20℃. The Power-law model (Eq. 1) was employed to fit the apparent viscosity-shear rate data as follows (Alghooneh, Razavi, & Behrouzian, 2017):

$$\eta_a = k\dot{\gamma}^{(n-1)} \quad (1)$$

where η_a is the apparent viscosity (Pa.s), $\dot{\gamma}$ is the shear rate (s^{-1}), k is the consistency coefficient ($Pa.s^n$) and n is the flow behavior index (no dimension).

Small dynamic oscillatory shear tests

Amplitude sweep test

The strain sweep test was performed in the range of 0.1 to 1000% and at a frequency of 1 Hz. The studied parameters were: elastic modulus (G'_{LVE}, Pa), loss modulus (G''_{LVE}, Pa), loss tangent ($\mathrm{Tan}\,\delta_{LVE}$, dimensionless) in the linear viscoelastic range (LVE), strain limiting value (γ_L, dimensionless), flow-point stress (τ_F, Pa) and modulus at the crossover point (G_f: $G' = G''$, Pa) (Behrouzian & Razavi, 2020).

Frequency sweep test

The frequency sweep assay was performed at a frequency range of 0.1-100 Hz within the LVE range ($\gamma = 0.5\%$). Using the power-law models, the acquired mechanical spectra were examined to determine the frequency dependence of storage modulus (G', Pa) (Eq. 2) and loss modulus (G'', Pa) (Eq. 3) (Behrouzian & Razavi, 2020):

$$G' = k'\omega^{n'} \quad (2)$$

$$G'' = k''\omega^{n''} \quad (3)$$

where k' ($Pa.s^n$) and k'' ($Pa.s^n$) are intercepts, n' and n'' are slopes of $log\, G'$ or $G''\ vs\ log\, \omega$ and ω is the angular frequency (Hz). The k''/k' (dimensionless), which is a measure of the relative contribution of the viscous component to the elastic component of EFGs, and the slope (η^*_s) of complex dynamic viscosity (η^*, Pa.s) *vs.* frequency were also calculated.

Furthermore, the following equation was used to calculate the network strength of EFGs (A, $Pa.s^{1/z}$) and the network extension (z, dimensionless) (Alghooneh, Razavi, & Kasapis, 2018; Khubber, Chaturvedi, Thakur, Sharma, & Yadav, 2021):

$$G^* = A \times \omega^{1/z} \quad (4)$$

where G^* is the complex modulus (Pa).

Large strain (fracture) rheological measurements

The EFGs were cut to form a cylindrical shape (20 mm in diameter and 20 mm in height) by using a cylindrical cutting mold. A uniaxial compression test was performed at 20-22℃ using a Texture Analyzer (CT3, Brookfield Ltd., USA) with a 10 kg load cell. The EFGs were compressed using a cylindrical probe (50 mm in diameter) with a constant deformation speed of 1 mm/s and a trigger load of 0.05 N to a target strain of 80%. The following equations were used to determine the true fracture stress (σ_T) (Eq. 5) and true fracture strain (ε_T) (Eq. 6) (Luo, Ye, Wolber, & Singh, 2020):

$$\sigma_T = \frac{F(t) \times H(t)}{H_0 \times A_0} \quad (5)$$

$$\varepsilon_T = -\ln\left(\frac{H(t)}{H_0}\right) \quad (6)$$

where $F(t)$ is the force at time t, $H(t)$ is the height at time t, A_0 and H_0 are the initial area and height of the EFGs, respectively. The fracture stress and fracture strain were determined from the point at which the true stress exhibits a first inflection in the curves. The fracture energy was calculated from the area under the stress-strain curve until the fracture point (Luo *et al*., 2020). Also, the slope of the linear section in the true stress-true strain curve was used to calculate the initial tangent modulus (I.T.M). The uniaxial compression test was performed in triplicate.

Held water determination

Held water was assigned by applying a microcentrifuge as adapted from Çakır & Foegeding (2011). This experiment was

conducted using a microcentrifuge filtration unit consisting of an inner spin tube and a 2 mL Eppendorf tube (Axygen Biosciences, Inc., Union City, USA). EFGs were cut into cylindrical forms of 10 mm in height and 4.8 mm in diameter using a metal cork borer. Then, by using a micro spatula, gel pieces were placed at the end of the spin tube, which was coated with filter paper with a diameter of 5.5 mm to diminish the grid size. Centrifugation was done at 600 × g for 10 min at 20 ℃. This investigation employed a 600 × g centrifugation force since no serum could be expulsed from the EFGs at lower forces than those reported by Çakır & Foegeding (2011) (153 × g). The amount of water released from the EFGs was measured by the weight of fluid gathered at the bottom of the Eppendorf tube. The held water was determined using the following equation:

$$Held\ water\ (\%) = \frac{W_T - W_g}{W_T} \times 100 \quad (7)$$

where W_T is the total amount of water in the samples (g) and W_g is the amount of water, which was eliminated from the EFGs during the test. The magnitude of W_T was determined by drying the samples in an oven at 105℃ for 10 h. Measurements were done for two samples of each treatment on two different days, and each prepared sample was replicated three times.

Data analysis

Analysis of variance (ANOVA) was used to determine significant differences (P<0.05) in all experimental data, and the Tukey test was used to compare the averages in Minitab 18. (Minitab Inc., Minneapolis, USA). Also, the curve fitting toolbox in MathWorks Matlab software (R2017b) was applied to fit the data.

Results and Discussion

Flow behavior

Figure 1 shows the viscosity of EFGs as a function of shear rate at various AG concentrations. As can be observed, the viscosity of EFGs decreases as the shear rate increased from 0.01 to 10 s-1. This can be linked to the progressive breakdown of their structures with increasing shear rate and their strong shear-thinning characteristic. Table 1 shows the rheological features of EFGs obtained by the Power-law model. With increasing AG content, the consistency coefficient (k) values rose considerably (P<0.05), ranging from 339.12 Pa.s^n in the control sample to 951.46 Pa.s^n in the 0.7% AG-contained sample. The capacity of the polymer chains of AG to form a three-dimensional structure is responsible for the increase in apparent viscosity of EFGs with increasing gum concentration. The flow behavior index (n) value in the control sample was 0.064. The magnitude of n decreased in the composite EFGs, with a value ranging from 0.023 to 0.039, which indicates the strong shear-thinning behavior of EFGs in the presence of AG. The low values obtained for n can be justified due to the large changes in apparent viscosity within a small range of shear rates (0.01-10 s^{-1}). For example, in the control sample, the magnitude of apparent viscosity decreased steeply from about 25,000 Pa.s at a shear rate of 0.01 to about 12.5 Pa.s at a shear rate of 10 s^{-1}, i.e., within this limited range of shear rate, the amount of apparent viscosity has been reduced by about 2000 times. Moreover, the reduction in viscosity with the shear rate for the sample containing 0.7% agar was more than 7500 times, indicating very shear-thinning behavior in the presence of agar. Similarly, Liu *et al*. (2022) reported that in the composite emulsion gel of WPI-sodium alginate formed using the layer-by-layer emulsion technique, the apparent viscosity was relatively large at low shear rates (about 86000 Pa.s at a shear rate of 0.1 s^{-1}) and decreased steeply with increasing shear rate (lower than 1000 Pa.s at a shear rate of 10 s^{-1}). A similar n value (0.019) was reported by Alavi, Emam-Djomeh, Mohammadian, Salami, & Moosavi-Movahedi (2020) for fibrillated egg white

proteins formed by the heating of protein solution at acidic conditions with an incubation time of 48 h. They stated that the long fibrils in this sample intensify the entanglement and disentanglement behaviors at low and high shear rates, respectively, resulting in a considerable shear-thinning feature in this sample.

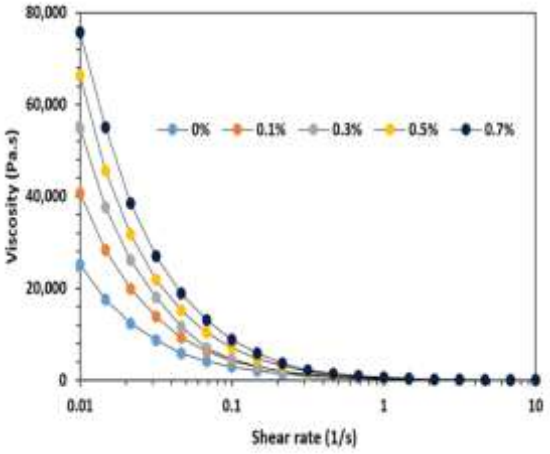

Fig. 1. Effect of AG concentration on the apparent viscosity of EFGs

Table 1. Steady shear rheological parameters of EFGs at different concentrations of agar gum (AG) based on the power-law model

AG (%)	$k\ (Pa.s^n)$	n (-)	R^2
0	339.12±24.03^{d}	0.064±0.005^{a}	0.999
0.1	489.27±38.06^{cd}	0.039±0.002^{b}	0.999
0.3	552.94 ±50.83^{c}	0.023±0.002^{c}	0.992
0.5	758.46 ±44.46^{b}	0.029±0.003^{bc}	0.999
0.7	951.46 ±53.82^{a}	0.039 ±0.006^{b}	0.993

All results were expressed as mean ± standard deviation values. Means in the same column followed by different letters are significantly different (Tukey test, P<0.05).

Dynamic rheological characteristics

Amplitude sweep test

As shown in Figure 2, an LVE zone in which G' and G'' were constant could be distinguished from a non-linear region in which G' and G'' began to drop with increasing strain and crossed over. Table 2 represents some key rheological characteristics obtained from the strain sweep test. The quantity of G'_{LVE} in the pure whey protein emulsion gel was 4438.3 Pa, and its value increased with an increase in the AG concentration; the highest value was recorded for 0.7% AG contained sample (23295.8 Pa). Therefore, EFGs strength increased with increasing the AG level. Also, the G''_{LVE} in the control sample was 751.40 Pa. When the AG concentration increased from 0.1 to 0.7%, its value increased from 1501.4 to 2694.8 Pa (Table 2). Tan δ_{LVE} is a key metric that describes the physical properties of gel systems and shows the ratio of G''_{LVE} to G'_{LVE} in each cycle. When the Tan δ_{LVE} value is more than 0.1 but less than 1, it indicates that an elastic structure exists in a weak biopolymer gel. To put it another way, the sample is not a genuine gel, and the structure is a cross between a highly concentrated biopolymer and a true gel (Naji-Tabasi & Razavi, 2017). The Tan δ_{LVE} in the pure whey protein emulsion gel sample was 0.17 (Table 2). The addition of AG considerably reduced the magnitude of Tan δ_{LVE} so that as the AG level increased from 0.1 to 0.7%, Tan δ_{LVE} decreased from 0.16 to 0.12, which indicates samples are moving closer to forming a true gel structure.

The γ_L shows the limiting value of strain, which after that G' decreases sharply. The γ_L represents the deformability of the sample structure and is dependent on the architecture of biopolymer molecules (Behrouzain & Razavi, 2020). The γ_L in the control sample was 2.53%. However, its value

decreased in the presence of AG and ranged from 1.28% (0.3% AG) to 1.9% (0.1% AG). An increase in AG concentration greater than 0.3% did not lead to a change in the γ_L value (P>0.05). This behavior reveals that when AG is present, the structure of EFGs becomes more vulnerable to minor deformations (Behrouzian & Razavi, 2020).

Another important parameter is the amount of stress at the crossover point (G'=G'') (τ_{f}, Pa), which represents the resistance to flow. After which, the network of gel structure is entirely disrupted, and flow behavior commences so that materials change from viscoelastic to elastoviscous behavior where the materials present irrecoverable deformation (Alghooneh et al., 2018; Hesarinejad, Koocheki, & Razavi, 2014). In the pure whey protein emulsion gel sample, the τ_{f} value was 327.76 Pa. In the composite EFGs, the τ_{f} rose from 460.17 to 812.34 Pa, as the AG content increased from 0.1 to 0.7%, respectively, which reflected increasing dynamic yield stress characteristics with increasing AG level (Table 2). The G_f displays the modulus value at the point where G' and G'' intersect. The magnitude of this parameter can be interpreted as a measure of the strength of the structure at the flow point (Naji-Tabasi & Razavi, 2017). The pure whey protein emulsion gel sample had a G_f value of 1053.40 Pa. In the composite samples, the G_f rose from 1761.22 at 0.1% AG to 3612.01 at 0.7% AG concentration.

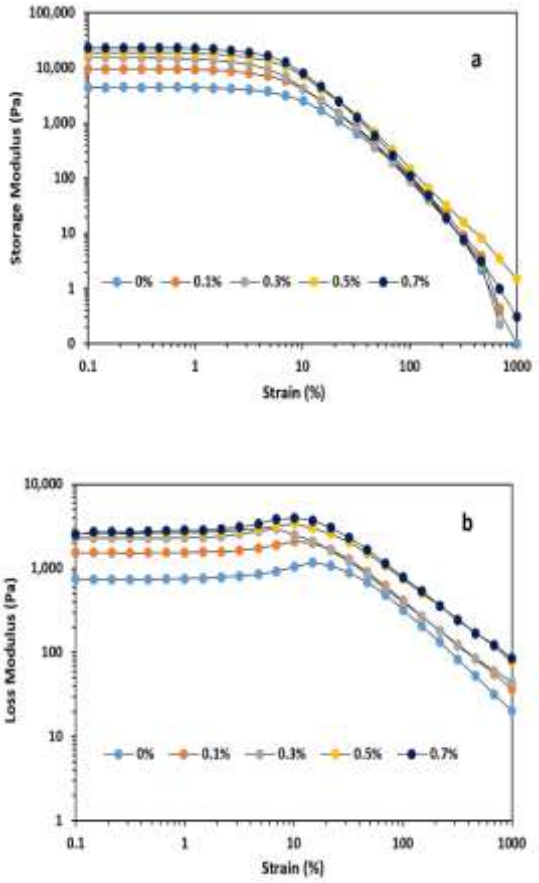

Fig. 2. Strain sweep dependency of storage modulus (G') (a) and loss modulus (G'') (b) of EFGs as a function of the AG concentration (strain range: 0.1-1000%, f=1 Hz, 20℃)

Table 2. Linear viscoelastic (LVE) parameters of emulsion filled gels (storage modulus $G'_{(\mathrm{LVE})}$, loss modulus $G''_{(\mathrm{LVE})}$, limiting value of strain (γ_L) loss-tangent value (Tan δ_{LVE}) in the linear viscoelastic range, and flow-point stress (τ_{f}) with the corresponding modulus G_{f}: $G' = G''$) (strain sweep test, f =1 Hz, 20℃)

AG (%)	$G'_{(\mathrm{LVE})}$(Pa)	$G''_{(\mathrm{LVE})}$(Pa)	γ_L(%)	Tan δ_{LVE}	τ_{f}(Pa)	G_{f}(Pa)
0	4438.3 ± 313.8^{e}	751.4 ± 53.1^{d}	2.53 ± 0.16 ^{a}	0.17 ± 0.01 ^{a}	327.76 ± 15.30 ^{d}	1053.40 ±59.59^{d}
0.1	9562.7 ± 540.9^{d}	1501.4 ±84.9^{c}	1.90 ± 0.08 ^{b}	0.16 ± 0.01^{ab}	460.17 ± 13.02 ^{c}	1761.22 ±99.63^{c}
0.3	15514.4±548.5^{c}	2293.7±81.1^{b}	1.28 ± 0.06^{cd}	0.15 ±0.01^{abc}	478.05 ± 40.56 ^{c}	1742.58±155.26^{c}
0.5	18987.5±749.3^{b}	2502.1±98.7^{ab}	1.47 ± 0.08^{bc}	0.13 ± 0.0 ^{bc}	674.78 ± 36.26 ^{b}	2573.46±145.58^{b}
0.7	23295.8±645.3^{a}	2694.8 ±74.7^{a}	1.42±0.12^{bcd}	0.12 ± 0.0 ^{c}	812.34 ± 28.72 ^{a}	3612.01±229.87^{a}

All results were expressed as mean ± standard deviation values. Means in the same column followed by different letters are significantly different (Tukey test, P<0.05).

After the γ_L limit, the material breaks, and the G' rapidly decreases. As a result, fracture data can be extracted from the strain sweep test. By plotting the result of

the elastic modulus and strain amplitude versus dynamic strain, fracture stress (τ_{Fr}) and fracture strain (γ_{Fr}) are determined from the peak point of the resulting graph. This approach is applicable to samples in which the complex modulus shows a peak value (Alghooneh *et al*., 2018). Table 3 shows the results of the τ_{Fr} and γ_{Fr} analysis. The γ_{Fr} in the pure whey protein emulsion gel was the highest (10.10%), indicating that this sample had the least sensitivity to entanglements at fracture point deformation. In the composite EFGs, the γ_{Fr} was in the range of 6.67 (0.3% AG) to 8.79% (0.1% AG). As evidenced in Table 3, the magnitudes τ_{Fr} in the composite emulsion gel were in the range of 389.37 Pa (0.3% AG) to 778.44 Pa (0.7% AG), which were significantly (P<0.05) higher than the control sample (255.22 Pa). This observation shows that composite gel samples have a more brittle structure in comparison to the control.

Table 3. Fracture stress (τ_{Fr}) and fracture strain (γ_{Fr}) of EFGs determined by amplitude sweep test

AG (%)	τ_{Fr} (Pa)	γ_{Fr} (%)
0	255.22 ± 12.62 ^{d}	10.10 ± 0.57 ^{a}
0.1	405.01 ± 16.61 ^{c}	8.79 ± 0.37 ^{a}
0.3	389.37 ± 14.06 ^{c}	6.67 ± 0.24 ^{b}
0.5	605.24 ± 18.83 ^{b}	6.79 ± 0.29 ^{b}
0.7	778.44 ± 26.42 ^{a}	6.83 ± 0.19 ^{b}

All results were expressed as mean ± standard deviation values. Means in the same column followed by different letters are significantly different (Tukey test, P<0.05).

Frequency sweep

Figure 3 displays the storage modulus (G') and loss modulus (G'') behaviors of prepared EFGs during the frequency sweep test. As shown, in all samples, there was no crossover between G' and G'', and G' values were significantly higher than G'' values over the applied frequency spectrum. Also, the magnitudes of both G' and G'' parameters were augmented by the increasing AG concentration. The power-law model (Eq. 2 and 3) was used to match the G' and G'' values *vs*. frequency to demonstrate the quantities of the network stiffness (k'), the consistency coefficient (k'') and the frequency dependence indicators (n' and n'') of the EFGs. As seen in Table 4, for all prepared EFGs, a high-coefficient degree of fitting was observed between frequency and G' and G'' values (R^2: 0.907-0.999). According to the statistical analysis, the AG concentration showed a significant impact on the k' and k'' parameters (P<0.05). In the pure whey protein emulsion gel, the magnitudes of k' and k'' were 5311.8 and 939.9 Pa, respectively. In the composite EFGs, by increasing the AG level, the k' and k'' values increased directly, and their values were in the range of 8555.9-25080.6 and 939.9-3574.9 Pa, respectively. The k'' to k' ratio (k''/k') can also represent the strength of gels. The more solid-like behavior of samples is shown by a larger increase in k' than k'' (Alghooneh *et al*., 2018). As appeared in Table 4, with increasing the AG concentration, the magnitude of k''/k' decreased obviously (P<0.05), from 0.18 in the control sample to 0.14 in the 0.7% AG-contained sample. These observations were in line with the strain sweep findings, that as the AG concentration was increased, the values of G'_{LVE} and G''_{LVE} increased and the magnitude of Tan δ_{LVE} of EFGs decreased. According to these results, adding AG to whey protein emulsion gel helps to generate a system with a more solid gel-like behavior, so that samples with a higher concentration of AG had a more compact gel network (Kazemi-Taskooh & Varidi, 2021; Yang et al., 2021).

The frequency dependency of G' and G'' (n' and n'') can also be used to characterize the viscoelastic properties of samples. The magnitudes n' and n''parameters are zero in fully elastic gels that do not show any frequency dependency, whereas n' and n'' values greater than zero denote frequency-dependent gels with less elasticity (Hesarinejad *et al.*, 2014; Wang *et al.*, 2020). As evidenced in Table 4, the quantities of n' and n'' of all the EFGs were in the range of 0.063–0.095 and 0.094–0.116, respectively. Also, as the AG level increased from 0.1 to 0.7% n' decreased considerably (P<0.05), but n'' did not show a significant change (P>0.05). Because solid behavior predominates, there is not expected to be a significant change in fluid-like behavior.

Another measure that can represent the strength of a gel is the slope of complex viscosity against frequency (η^*_s). A greater value of η^*_s implies that the gel is stronger (Naji-Tabasi & Razavi, 2017). By adding the AG, the absolute value of η^*_s increased (P>0.05) from their initial value (0.909), and its value was in the range of 0.918-0.936 (Table 4). A similar value was reported for AG gel (0.925) at a concentration of 1% at 25℃ (Alghooneh *et al.*, 2018).

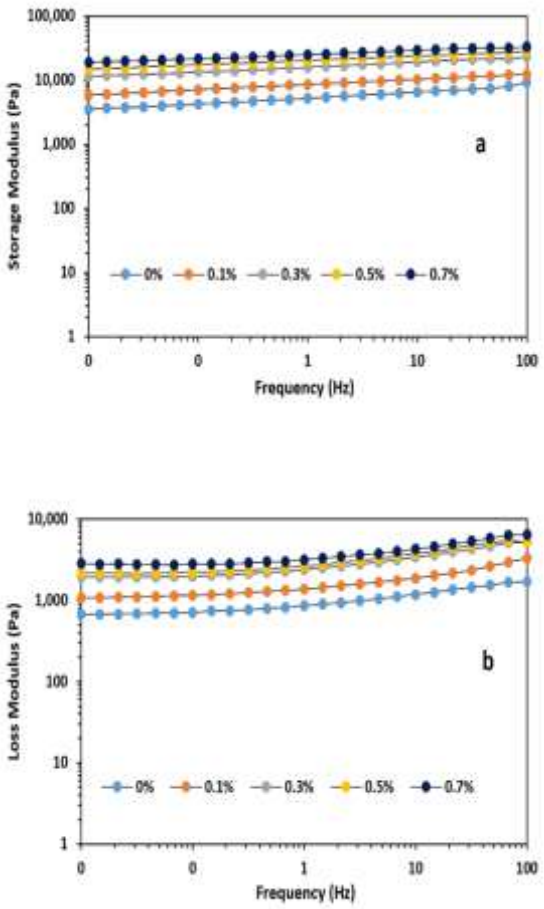

Fig. 3. Frequency sweep dependency of storage modulus (G') (a) and loss modulus (G'') (b) of EFGs as a function of the AG concentration (frequency range: 0.01-100 Hz, γ=0.5%, 20℃)

Table 4. Dynamic rheological parameters of emulsion-filled gels determined by the frequency sweep test (Strain sweep=0.5%, 20℃)

AG (%)	K'(Pa)	$n'(-)$	R^2	K''(Pa)	$n''(-)$	R^2	K''/K'	η^*_s
0	5311.8±187.8^{e}	0.095±0.005^{a}	0.988	939.9±33.2^{d}	0.116±0.009^{a}	0.934	0.18±0.01^{a}	-0.909±0.024^{a}
0.1	8555.9±302.5^{d}	0.081±0.002^{ab}	0.999	1534.1±54.2^{c}	0.113±0.008^{a}	0.908	0.18±0.01^{a}	-0.918±0.091^{a}
0.3	15992.1±5202^{c}	0.076±0.005^{ab}	0.997	2683.5±87.3^{b}	0.111±0.009^{a}	0.907	0.17±0.01^{ab}	-0.923±0.065^{a}
0.5	20338.3±8629^{b}	0.069±0.004^{b}	0.999	2961.7±1257 ^{b}	0.109±0.005^{a}	0.910	0.15±0.01^{b}	-0.931±0.072^{a}
0.7	25080.6±744.8 ^{a}	0.063±0.005^{b}	0.998	3574.9±1062 ^{a}	0.094±0.005^{a}	0.909	0.14±0.00^{b}	-0.936±0.053^{a}

All results were expressed as mean ± standard deviation values. Means in the same column followed by different letters are significantly different (Tukey test, P<0.05).

Establishing a link between the dynamic complex modulus (G^*, Pa) and the frequency (ω, rad/s) based on the Power-law model is recommended for displaying some relevant information about the connections of a 3D network and its macroscopic properties. The *z* parameter in this model is a measure of the extent of the network and is defined as a criterion of rheological unit numbers equated with each other in the 3D-network to create the food structure, and the *A* parameter

represents the strength of the contact between these units (Anvari & Joyner, 2017; Heydari & Razavi, 2021). In the control sample, the magnitudes of the *A* and *z* parameters were 5380.11 Pa.$s^{1/z}$ and 10.05, respectively (Table 5). As AG concentration increased, the values of *A* and *z* parameters increased meaningfully (P<0.05) from 8695.3 Pa.$s^{1/z}$ and 12.04 (0.1% AG) to 25344.3 Pa.$s^{1/z}$ and 15.59 (0.7% AG), respectively. Increasing the z value with increasing AG level suggested that AG increased the number of nodes and interacting strands of the whey protein emulsion gel network and the EFGs' network became more extensive. However, increasing coefficient *A* indicates that the magnitude of the interactions increased. Therefore, the 0.7% AG-WPI EFG sample has the most complex structure and the highest level of interactions between protein and polysaccharide. Alghooneh *et al* (2018) reported that the values of *A* and *z* parameters in the AG gel at a concentration of 1% at 25℃ were 5338.43 Pa.$s^{1/z}$ and 17.55, respectively.

Table 5. The strength of network (*A*) and the network extension (z) of EFGs at 20℃

AG (%)	A (Pa. $s^{1/z}$)	z (-)	R^2
0	5380.11±228.26^{e}	10.05±0.38^{d}	0.977
0.1	8695.32±368.91^{d}	12.04±0.51^{c}	0.999
0.3	16224.5±573.62^{c}	12.78±0.45^{bc}	0.996
0.5	20567.91±639.92^{b}	14.33±0.57^{ab}	0.999
0.7	25344.31±716.85^{a}	15.59 ±0.44^{a}	0.997

All results were expressed as mean ± standard deviation values. Means in the same column followed by different letters are significantly different (Tukey test, P<0.05).

Applicability of Cox–Merz rule

The *Cox-Merz* rule describes the correlation between dynamic and steady shear viscosity as follows (Cox & Merz, 1958):

$$\eta^*(\omega) = \eta_a(\dot{\gamma})\Big|_{\omega=\dot{\gamma}} \quad (8)$$

Based on this rule, the η^* at a particular ω is equivalent to η_a at a particular $\dot{\gamma}$, when $\omega = \dot{\gamma}$. This rule is extremely beneficial because the utilization of high shear stress conditions in a wide range of polymeric systems causes a fracture in the sample and secondary flows, making steady viscosity measurement more challenging, and also, dynamic shear data is easier to collect using automated rheometers than steady shear data (Rao & Cooley, 1992; Sagdic, Toker, Polat, Arici, & Yilmaz, 2015). Furthermore, by using this rule, some data on the microstructure of food products can be obtained. When there is no substantial engagement between biopolymer chains, the dynamic and steady shear flow patterns are identical. Deviation from the *Cox-Merz* rule, on the other hand, might indicate a high level of strong intermolecular and intramolecular interactions (Sagdic *et al*., 2015). Therefore, this criterion is not followed by systems with gel-like behavior due to regular chains and tight conformation, as displayed in Figure 4, where the complex viscosity (η^*) was larger than the apparent viscosity (η_a) in all samples, which the structural decay caused by steady shear deformation was the cause of this. In oscillatory shear, the deformation effect is low, but it is large enough in steady shear to break down intermolecular connections (Razavi, Alghooneh, & Behrouzian, 2018).

The greater the deviation from this rule, the greater the strength of the network (Karaman *et al*., 2013). Calculating the difference between integrals of the complex viscosity (η^*)-angular velocity (ω) and the apparent viscosity (η_a)-shear rate ($\dot{\gamma}$) curves can be used to determine the extent of divergence (φ) from the *Cox-Merz* rule (Alghooneh *et al*., 2017):

$$\varphi = abs\left(\int_{\omega_0}^{\omega} \eta^* d\omega - \int_{\dot{\gamma}_0}^{\dot{\gamma}} \eta_a d\dot{\gamma}\right) \quad (9)$$

As seen in Table 6, by utilizing AG, the φ value of the EFGs increased significantly (P<0.05), from 3476.80 Pa in the control sample to 21509.44 Pa in the 0.7% AG contained sample, which represents the formation of stronger structures by adding AG. Alghooneh *et al*. (2018) reported that the magnitude of the φ parameter in the AG gel at a concentration of 1% at 25℃ was 39317.707 Pa.

As shown in Figure 4, the complex viscosity (η^*) was larger than the apparent viscosity (η_a) were almost parallel to each other over the whole range of the angular frequency or shear rates. Therefore, steady shear viscosity can be estimated by applying dynamic shear data and the gained shift factor, and vice-versa, at an equal frequency and shear rate (Karaman *et al*., 2013). For this purpose, the modified Cox-Merz rule can be used to alter the difference between the dynamic and steady shear viscosities as follows (Alghooneh *et al*., 2017; Kurt, Cengiz, & Kahyaoglu, 2016):

$$\eta^*(\omega) = \eta(\alpha\dot{\gamma}) \quad (10)$$

where, α represents the shift factor. As evidenced in Table 6, by increasing the AG level, the magnitude of α increased, and the highest and the lowest quantities of α were related to the 0.7% AG-contained sample (3.96) and the pure whey protein emulsion gel sample (2.29), respectively.

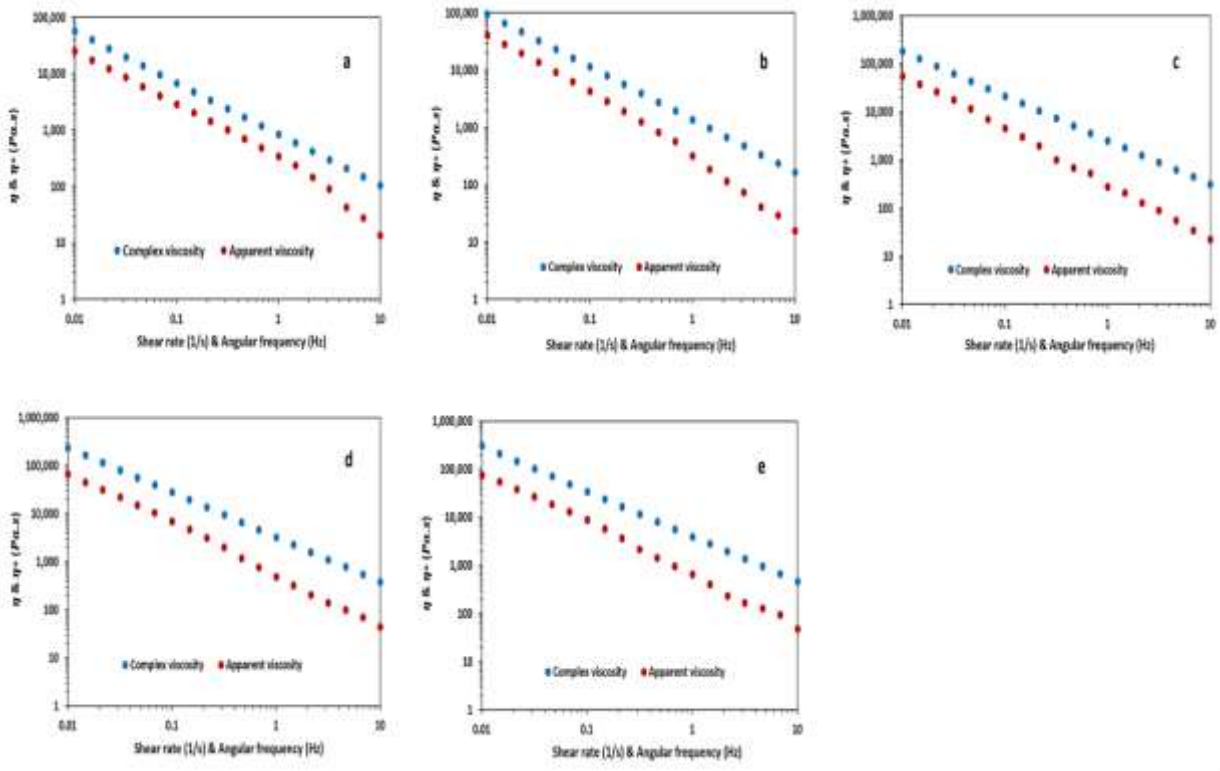

Fig. 4. Comparison of the complex viscosity (η^*) and apparent viscosity (*Cox–Merz* rule) for control sample (a), and 0.1% AG (b), 0.3% AG (c), 0.5% AG (d) and 0.7% AG (e) contained samples

Table 6. The extent of departure (φ) and shift factor (α) for EFGs at 20℃

AG (%)	φ (Pa)	α (-)
0	3476.80 ± 344.19 ^{c}	2.29 ± 0.08 ^{c}
0.1	6491.57 ± 550.83 ^{c}	2.36 ± 0.10 ^{c}
0.3	14034.35 ± 793.90 ^{b}	3.44 ± 0.12 ^{b}
0.5	17346.92 ± 1103.95 ^{b}	3.64 ± 0.17 ^{ab}
0.7	21509.44 ± 1216.76 ^{a}	3.96 ± 0.11 ^{a}

All results were expressed as mean ± standard deviation values. Means in the same column followed by different letters are significantly different (Tukey test, P<0.05).

Textural characteristics

Initial tangent modulus

As evidenced in Table 7, by utilizing AG, the initial tangent modulus (I.T.M) increased significantly (P<0.05), and its value was in the range of 23.22 kPa in the control sample to 112.34 kPa in the 0.7% AG-contained sample, which simply signifies the stiffer structure of the prepared EFGs in the presence of AG, especially at higher concentrations (Oliver, Scholten, & van Aken, 2015). Local concentration and connectivity among protein aggregates increased as polysaccharide content rose, which could explain why the gels became stiffer (Munialo *et al*., 2016). According to de Jong and van de Velde (2007), in mixed gels of whey proteins and polysaccharides with various charge densities generated via acid-induced cold gelation, the number of effective strands and the modulus of the strands are proportional to the gel modulus.

Fracture stress

This parameter is an index of gel hardness (Vilela *et al*., 2011). As seen in Table 7, the AG concentration had a significant impact on the true fracture stress (σ_T) of the EFGs. According to the given data, with increasing the AG level, the magnitude of σ_T increased directly and its value was in the range of 10.39 kPa in the pure whey protein emulsion gel sample to 27.21 kPa in the 0.7% AG-contained sample. In general, the acquired values for σ_T were in line with the values of τ_{Fr} extracted from the amplitude sweep test (Table 3). In the composite gels, the rise in gel hardness might arise from a reduction in porosity and an increase in hydrogel network homogeneity (Babaei, Mohammadian, & Madadlou, 2019; Jang & Matsubara, 2005), and increasing the local concentration and connectivity between protein aggregates (Çakır & Foegeding, 2011).

Fracture strain

The fracture strain is a reflection of the weakest point in the solid-phase spatial network and can be considered as a measure of the gel deformability (Munialo *et al*., 2016; Vilela *et al*., 2011). In the control sample, the true fracture strain (ε_T) was 0.57 (Table 7). ε_T in the 0.1% AG-contained sample (0.56) was equal to the pure whey protein emulsion gel (P>0.05). The outputs of the ε_T analysis demonstrated that by elevating the AG concentration to 0.3%, ε_T decreased meaningfully (P<0.05) (0.30). But there was not a considerable difference between the ε_T values of 0.3, 0.5, and 0.7% AG-contained samples (P>0.05). In similar, Vilela *et al*. (2011) found that in the mixed gels of soy protein isolate-gellan gum, the fracture strain was independent of an increase in polysaccharide concentration from 0.3 to 0.7%, demonstrating that this feature was only controlled by the type of interaction occurring between the protein and the polysaccharide.

Fracture energy

Fracture energy is computed as the quantity of energy required to compress the sample to the point of fracture. As provided in Table 7, statistical analysis revealed that the quantity of fracture

energy in the AG concentrations of 0.1% (30.07 mJ), 0.5% (24.37 mJ), and 0.7% (26.13 mJ) was similar to that of the control sample (24.65 mJ) (P>0.05). The EFG containing 0.3% AG sample required considerably (P<0.05) low fracture energy (13.84 mJ). Gels having lower fracture energy are easier to break down into small fragments in the mouth and need fewer chewing cycles Luo *et al*. (2020).

Table 7. Mechanical properties of emulsion filled gels measured by the uniaxial compression test

AG (%)	Initial tangent modulus (kPa)	True fracture stress (kPa)	True fracture strain (-)	Fracture energy (mJ)
0	23.22 ± 1.16 ^{e}	10.39 ± 0.83 ^{d}	0.57 ± 0.04 ^{a}	24.65 ± 2.97 ^{ab}
0.1	28.39 ± 2.03 ^{d}	12.34 ± 0.77 ^{c}	0.56 ± 0.03 ^{a}	30.07 ± 3.81 ^{a}
0.3	62.08 ± 3.04 ^{c}	13.30 ± 1.42 ^{c}	0.30 ± 0.03 ^{b}	13.84 ± 2.84 ^{b}
0.5	96.67 ± 2.97 ^{b}	22.99 ± 1.18 ^{b}	0.29 ± 0.02 ^{b}	24.37 ± 3.37 ^{ab}
0.7	112.34 ± 4.09 ^{a}	27.21 ± 1.59 ^{a}	0.28 ± 0.03 ^{b}	26.13 ± 3.21 ^{ab}

All results were expressed as mean ± standard deviation values. Means in the same column followed by different letters are significantly different (Tukey test, P<0.05).

Held water

Held water is a basic measure that represents the fraction of total moisture that is held by the gel network under a given force. The amount of serum released under the mechanical force applied to the gel during centrifugation represents the amount of released serum from the gel during mastication. (Devezeaux de Lavergne, Strijbosch, Van den Broek, Van de Velde, & Stieger, 2016; Çakır & Foegeding, 2011; Gwartney, Larick, & Foegeding, 2004). Figure 5 displays the held water of EFGs as a function of AG concentration. The amount of held water in the pure whey protein emulsion gel sample was 75.49%. Results showed that the addition of AG at a low level did not considerably affect the magnitude of held water. But high AG concentration meaningfully decreased the held water of the EFGs and the lowest value of held water was found in the sample containing 0.7% AG (60.97%). Our findings were in line with the reported data by Zhang and Vardhanabhuti (2014), Çakır & Foegeding (2011), and van den Berg, van Vliet, vander Linden, van Boekel, & van de Velde (2007), where they stated that the water holding capacity of WPI/pectin, WPI/*k*-carrageenan, and WPI/gellan mixed gels decreased respectively by increasing the concentration of polysaccharide. They stated that the differences in the capacity of these mixed gels to hold the aqueous phase in their network during centrifugation correspond to the differences in the protein-polysaccharide interactions and microstructure features so that as the polysaccharide concentration increased, a change in microstructure from homogenous in the pure WPI gel to bicontinuous in the mixed gels was observed. In these researches, it is stated that the porosity was considerably lower in the protein continuous gels, and the aqueous phase was entrapped in spheres formed throughout the protein network. Therefore, gels can hold the aqueous phase in their network during centrifugation. However, the addition of polysaccharides resulted in a considerable reduction in water-holding capacity, corresponding to a shift in microstructure to bicontinuous, where bigger channels penetrated the protein phase, allowing for enhanced fluid movement.

The higher water release during oral processing can have a positive effect on taste and aroma perception. Costell, Peyrolon, and Duran (2000) found that sweetness and saltiness intensities in gellan gels were higher than in *k*-carrageenan gels with the same strength, indicating that different hydrocolloids have different tastant release properties. The authors proposed that the higher amount of water released by gellan gels during mastication is the cause of these variations. Moreover, as stated in section 2.6, in all the prepared

EFGs, almost no water was excluded at lower forces and the held water was close to 100% (data not shown), which can be expected that the EFGs have low serum release during storage.

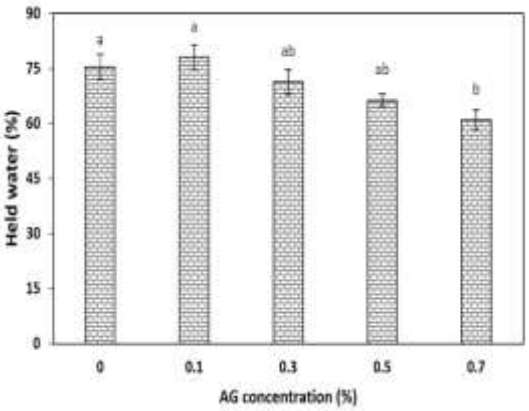

Fig. 5. Effect of AG concentration on the held water of EFGs. Mean values with different letters differ significantly (P<0.05).

Conclusions

Adding AG had a variety of consequences for the WPI-AG composite EFGs. The apparent viscosity, elastic modulus (G'_{LVE}), loss modulus (G''_{LVE}), flow-point stress (τ_F,), k', k'', network strength (A), network extension (z), the extent of departure from the *Cox-Merz* rule (φ), and initial tangent modulus (I.T.M), all increased as the AG level increased from 0.1 to 0.7% w/w, whereas the held water decreased. A low concentration of AG (0.1%) had no significant effect on the fracture strain, while at concentrations of 0.3 to 0.7%, the fracture strain was significantly lower than the control sample. The highest value of the fracture stress of the EFGs was related to the 0.7% AG-contained sample, which had equal fracture energy to the pure whey protein emulsion gel sample. Also, in the composite AG-WPI samples, the lowest values of fracture energy, flow behavior index, the linear limit of strain, and modulus at the crossover point (in the strain sweep assay) were recorded for the 0.3% AG-contained sample. Overall, the addition of AG can have positive effects on the rheo-mechanical features and oral processing behaviors of whey protein-based EFGs so that it is feasible to produce composite EFGs with higher strength in the presence of AG, which could provide a good delivery system for enhancing bioavailability and stability of functional components during storage. Also, composite AG-WPI EFGs are expected to exhibit favorable fracture behavior during oral processing due to their lower fracture energy and fracture strain.

Acknowledgments

The Ferdowsi University of Mashhad (FUM) financial support is sincerely thanked (Grant No. 49939). The authors are also grateful to Agropur Ingredients Co. (Le Sueur, MN, USA) and their sales manager, Mr. Yves Schellenberg, for donating whey protein isolate.

References

Alavi, F., Emam-Djomeh, Z., Mohammadian, M., Salami, M., & Moosavi-Movahedi, A. A. (2020). Physico-chemical and foaming properties of nanofibrillated egg white protein and its functionality in meringue batter. *Food Hydrocolloids*, *101*, 105554. doi: https://doi.org/10.1016/j.foodhyd.2019.1055543

Alavi, F., Momen, S., Emam-Djomeh, Z., Salami, M., & Moosavi-Movahedi, A. A. (2018). Radical cross-linked whey protein aggregates as building blocks of non-heated cold-set gels. *Food Hydrocolloids*, *81*, 429-441. doi: https://doi.org/10.1016/j.foodhyd.2018.03.016

Alghooneh, A., Razavi, S. M. A., & Behrouzian, F. (2017). Rheological characterization of hydrocolloids interaction: A case study on sage seed gum-xanthan blends. *Food Hydrocolloids*, 66, 206-215. doi: https://doi.org/10.1016/j.foodhyd.2016.11.022

Alghooneh, A., Razavi, S. M., & Kasapis, S. (2018). Hydrocolloid clustering based on their rheological properties. *Journal of Texture Studies*, *49*(6), 619-638. doi: https://doi.org/10.1111/jtxs.12368

Anvari, M., & Joyner, H. S. (2017). Effect of fish gelatin-gum arabic interactions on structural and functional properties of concentrated emulsions. *Food Research International*, *102*, 1-7. doi: https://doi.org/10.1016/j.foodres.2017.09.085

Babaei, J., Mohammadian, M., & Madadlou, A. (2019). Gelatin as texture modifier and porogen in egg white hydrogel. *Food Chemistry*, *270*, 189-195. doi: https://doi.org/10.1016/j.foodchem.2018.07.109

Behrouzain, F., & Razavi, S. M. (2020). Structure-rheology relationship of basil seed gum-whey protein isolate mixture: Effect of thermal treatment and biopolymer ratio. *Food Hydrocolloids*, *102*, 105608. doi: https://doi.org/10.1016/j.foodhyd.2019.105608

Behrouzain, F., Razavi, S. M., & Joyner, H. (2020). Mechanisms of whey protein isolate interaction with basil seed gum: Influence of pH and protein-polysaccharide ratio. *Carbohydrate Polymers*, *232*, 115775. doi: https://doi.org/10.1016/j.carbpol.2019.115775

Çakır, E., & Foegeding, E. A. (2011). Combining protein micro-phase separation and protein–polysaccharide segregative phase separation to produce gel structures. *Food Hydrocolloids*, *25*(6), 1538-1546. doi: https://doi.org/10.1016/j.foodhyd.2011.02.002

Chaux-Gutiérrez, A. M., Pérez-Monterroza, E. J., & Mauro, M. A. (2019). Rheological and structural characterization of gels from albumin and low methoxyl amidated pectin mixtures. *Food Hydrocolloids*, *92*, 60-68. doi: https://doi.org/10.1016/j.foodhyd.2019.01.025

Costell, E., Peyrolon, M., & Duran, L. (2000). Note. Influence of texture and type of hydrocolloid on perception of basic tastes in carrageenan and gellan gels. *Food Science and Technology International*, *6*(6), 495-499. doi: https://doi.org/10.1177/108201320000600608

Cox, W. P., & Merz, E. H. (1958). Correlation of dynamic and steady flow viscosities. *Journal of Polymer Science*, *28*, 619-622. doi: https://doi.org/10.1002/pol.1958.1202811812

de Jong, S., & van de Velde, F. (2007). Charge density of polysaccharide controls microstructure and large deformation properties of mixed gels. *Food Hydrocolloids*, *21*(7), 1172-1187. doi: https://doi.org/10.1016/j.foodhyd.2006.09.004

Devezeaux de Lavergne, M., Strijbosch, V. M., Van den Broek, A. W., Van de Velde, F., & Stieger, M. (2016). Uncoupling the impact of fracture properties and composition on sensory perception of emulsion-filled gels. *Journal of Texture Studies*, *47*(2), 92-111. doi: https://doi.org/10.1111/jtxs.12164

Farjami, T., & Madadlou, A. (2019). An overview on preparation of emulsion-filled gels and emulsion particulate gels. *Trends in Food Science & Technology*, *86*, 85-94. doi: https://doi.org/10.1016/j.tifs.2019.02.043

Gwartney, E. A., Larick, D. K., & Foegeding, E. A. (2004). Sensory texture and mechanical properties of stranded and particulate whey protein emulsion gels. *Journal of food science*, *69*(9), S333-S339. doi: https://doi.org/10.1111/j.1365-2621.2004.tb09945.x

Hesarinejad, M. A., Koocheki, A., & Razavi, S. M. A. (2014). Dynamic rheological properties of *Lepidium perfoliatum* seed gum: Effect of concentration, temperature and heating/cooling rate. *Food Hydrocolloids*, *35*, 583-589. doi: https://doi.org/10.1016/j.foodhyd.2013.07.017

Heydari, A., & Razavi, S. M. A. (2021). Evaluating high pressure-treated corn and waxy corn starches as novel fat replacers in model low-fat O/W emulsions: A physical and rheological study. *International Journal of Biological Macromolecules*, *184*, 393-404. doi: https://doi.org/10.1016/j.ijbiomac.2021.06.052

Jang, B. K., & Matsubara, H. (2005). Influence of porosity on hardness and Young's modulus of nanoporous EB-PVD TBCs by nanoindentation. *Materials Letters*, *59*(27), 3462-3466. doi: https://doi.org/10.1016/j.matlet.2005.06.014

Karaman, S., Yilmaz, M. T., & Kayacier, A. (2013). Mathematical approach for two component modeling of salep–starch mixtures using central composite rotatable design: Part II. Dynamic oscillatory shear properties and applicability of *Cox–Merz* rule. *Food Hydrocolloids*, *31*(2), 277-288. doi: https://doi.org/10.1016/j.foodhyd.2012.10.002

Kazemi-Taskooh, Z., & Varidi, M. (2021). Designation and characterization of cold-set whey protein-gellan gum hydrogel for iron entrapment. *Food Hydrocolloids*, *111*, 106205. doi: https://doi.org/10.1016/j.foodhyd.2020.106205

Khalesi, H., Emadzadeh, B., Kadkhodaee, R., & Fang, Y. (2019). Effect of Persian gum on whey protein concentrate cold-set emulsion gel: Structure and rheology study. *International Journal of Biological Macromolecules*, *125*, 17-26. doi: https://doi.org/10.1016/j.foodhyd.2020.106205

Khubber, S., Chaturvedi, K., Thakur, N., Sharma, N., & Yadav, S. K. (2021). Low-methoxyl pectin stabilizes low-fat set yoghurt and improves their physicochemical properties, rheology, microstructure and sensory liking. *Food Hydrocolloids*, *111*, 106240. doi: https://doi.org/10.1016/j.foodhyd.2020.106240

Kurt, A., Cengiz, A., & Kahyaoglu, T. (2016). The effect of gum tragacanth on the rheological properties of salep based ice cream mix. *Carbohydrate Polymers*, *143*, 116-123. doi: https://doi.org/10.1016/j.carbpol.2016.02.018

Li, R., Cheng, Y., Tang, N., Wu, L., Nirasawa, S., Jia, X., & Cao, W. (2020). Rheological, structural and physicochemical characteristics of heat-induced egg albumin/sesbania gum mixed gels. *International Journal of Biological Macromolecules*, *163*, 87-95. doi: https://doi.org/10.1016/j.ijbiomac.2020.06.172

Liu, F., Liang, X., Yan, J., Zhao, S., Li, S., Liu, X., ... & McClements, D. J. (2022). Tailoring the properties of double-crosslinked emulsion gels using structural design principles: Physical characteristics, stability, and delivery of lycopene. *Biomaterials*, *280*, 121265. doi: https://doi.org/10.1016/j.biomaterials.2021.121265

Lu, Y., Mao, L., Hou, Z., Miao, S., & Gao, Y. (2019). Development of emulsion gels for the delivery of functional food ingredients: From structure to functionality. *Food Engineering Reviews*, *11*(4), 245-258. doi: https://doi.org/10.1007/s12393-019-09194-z

Luo, N., Ye, A., Wolber, F. M., & Singh, H. (2020). In-mouth breakdown behaviour and sensory perception of emulsion gels containing active or inactive filler particles loaded with capsaicinoids. *Food Hydrocolloids*, *108*, 106076. doi: https://doi.org/10.1016/j.foodhyd.2020.106076

Mao, L., Miao, S., Yuan, F., & Gao, Y. (2018). Study on the textural and volatile characteristics of emulsion filled protein gels as influenced by different fat substitutes. *Food Research International*, *103*, 1-7. doi: https://doi.org/10.1016/j.foodres.2017.10.024

Munialo, C. D., van der Linden, E., Ako, K., Nieuwland, M., Van As, H., & de Jongh, H. H. (2016). The effect of polysaccharides on the ability of whey protein gels to either store or dissipate energy upon mechanical deformation. *Food Hydrocolloids*, *52*, 707-720. doi: https://doi.org/10.1016/j.foodhyd.2015.08.013

Naji-Tabasi, S., & Razavi, S. M. A. (2017). New studies on basil (*Ocimum bacilicum* L.) seed gum: Part III–Steady and dynamic shear rheology. *Food Hydrocolloids*, *67*, 243-250. doi: https://doi.org/10.1016/j.foodhyd.2015.12.020

Oliver, L., Scholten, E., & van Aken, G. A. (2015). Effect of fat hardness on large deformation rheology of emulsion-filled gels. *Food Hydrocolloids*, *43*, 299-310. doi: https://doi.org/10.1016/j.foodhyd.2014.05.031

Pandey, S., Senthilguru, K., Uvanesh, K., Sagiri, S. S., Behera, B., Babu, N., & Banerjee, I. (2016). Natural gum modified emulsion gel as single carrier for the oral delivery of probiotic-drug combination. *International Journal of Biological Macromolecules*, *92*, 504-514. doi: https://doi.org/10.1016/j.ijbiomac.2016.07.053

Rao, M. A., & Cooley, H. J. (1992). Rheological behavior of tomato pastes in steady and dynamic shear. *Journal of Texture Studies*, *23*(4), 415-425. doi: https://doi.org/10.1111/j.1745-4603.1992.tb00031.x

Razavi, S. M., Alghooneh, A., & Behrouzian, F. (2018). Influence of temperature on sage seed gum (*Salvia macrosiphon*) rheology in dilute and concentrated regimes. *Journal of Dispersion Science and Technology*, *39*, 982-995. doi: https://doi.org/10.1080/01932691.2017.1379020

Sagdic, O., Toker, O. S., Polat, B., Arici, M., & Yilmaz, M. T. (2015). Bioactive and rheological properties of rose hip marmalade. *Journal of Food Science and Technology*, *52*(10), 6465-6474. doi: https://doi.org/10.1007/s13197-015-1753-z

Sow, L. C., Tan, S. J., & Yang, H. (2019). Rheological properties and structure modification in liquid and gel of tilapia skin gelatin by the addition of low acyl gellan. *Food Hydrocolloids*, *90*, 9-18. doi: https://doi.org/10.1016/j.foodhyd.2018.12.006

Torres, O., Murray, B., & Sarkar, A. (2016). Emulsion microgel particles: Novel encapsulation strategy for lipophilic molecules. *Trends in Food Science & Technology*, *55*, 98-108. doi: https://doi.org/10.1016/j.tifs.2016.07.006

Van den Berg, L., Van Vliet, T., Van der Linden, E., Van Boekel, M. A. J. S., & Van de Velde, F. (2007). Serum release: the hidden quality in fracturing composites. *Food Hydrocolloids*, *21*(3), 420-432. doi: https://doi.org/10.1016/j.foodhyd.2006.05.002

Vilela, J. A. P., Cavallieri, Â. L. F., & Da Cunha, R. L. (2011). The influence of gelation rate on the physical properties/structure of salt-induced gels of soy protein isolate–gellan gum. *Food Hydrocolloids*, *25*(7), 1710-1718. doi: https://doi.org/10.1016/j.foodhyd.2011.03.012

Wang, W., Shen, M., Jiang, L., Song, Q., Liu, S., & Xie, J. (2020). Influence of *Mesona blumes* polysaccharide on the gel properties and microstructure of acid-induced soy protein isolate gels. *Food Chemistry*, *313*, 126125. doi: https://doi.org/10.1016/j.foodchem.2019.126125

Xiong, W., Ren, C., Tian, M., Yang, X., Li, J., & Li, B. (2017). Complex coacervation of ovalbumin-carboxymethylcellulose assessed by isothermal titration calorimeter and rheology: Effect of ionic strength and charge density of polysaccharide. *Food Hydrocolloids*, *73*, 41-50. doi: https://doi.org/10.1016/j.foodhyd.2017.06.031

Yang, Q., Wang, Y. R., Li-Sha, Y. J., & Chen, H. Q. (2021). The effects of basil seed gum on the physicochemical and structural properties of arachin gel. *Food Hydrocolloids*, *110*, 106189. doi: https://doi.org/10.1016/j.foodhyd.2020.106189

Zhang, C., An, D., Xiao, Q., Weng, H., Zhang, Y., Yang, Q., & Xiao, A. (2020). Preparation, characterization, and modification mechanism of agar treated with hydrogen peroxide at different temperatures. *Food Hydrocolloids*, *101*, 105527. doi: https://doi.org/10.1016/j.foodhyd.2019.105527

Zhang, S., & Vardhanabhuti, B. (2014). Acid-induced gelation properties of heated whey protein− pectin soluble complex (Part II): Effect of charge density of pectin. *Food Hydrocolloids*, *39*, 95-103. doi: https://doi.org/10.1016/j.foodhyd.2013.12.020

Zhao, H., Chen, J., Hemar, Y., & Cui, B. (2020). Improvement of the rheological and textural properties of calcium sulfate-induced soy protein isolate gels by the incorporation of different polysaccharides. *Food Chemistry*, *310*, 125983. doi: https://doi.org/10.1016/j.foodchem.2019.125983

Zheng, H., Beamer, S. K., Matak, K. E., & Jaczynski, J. (2019). Effect of κ-carrageenan on gelation and gel characteristics of Antarctic krill (*Euphausia superba*) protein isolated with isoelectric solubilization/precipitation. *Food Chemistry*, *278*, 644-652. doi: https://doi.org/10.1016/j.foodchem.2018.11.080

ارزیابی اثرات صمغ آگار بر خواص بافتی و رئولوژیکی ژل سرد پر شده امولسیونی ایزوله پروتئین آب پنیر

محمّد رضا صلاحی [۱]، سید محمّد علی رضوی [۲*]، محبّت محبّی [۲]

۱- دانشجوی دکتری، گروه علوم و صنایع غذایی، دانشگاه فردوسی مشهد، مشهد، ایران
۲- استاد، گروه علوم و صنایع غذایی، دانشگاه فردوسی مشهد، مشهد، ایران
* نویسنده مسئول (s.razavi@um.ac.ir)

چکیده

در این پژوهش تاثیر صمغ آگار (۰/۷-۰ درصد) بر ویژگی‌های بافتی، رئولوژیکی و ظرفیت نگه داری آب ژل سرد پر شده امولسیونی ایزوله پروتئین آب پنیر مورد بررسی قرار گرفت. نتایج آزمون برشی پایا نشان داد که تمامی نمونه‌ها دارای رفتار شل شونده با برش هستند و با افزایش غلظت آگار، مقدار ضریب قوام از ۳۳۹/۱۲ پاسکال.ثانیه در نمونه شاهد تا ۹۵۱/۴۶ پاسکال.ثانیه در نمونه حاوی ۰/۷ درصد آگار افزایش یافت. در آزمون کرنش متغیر، غلظت آگار تاثیر معنی داری بر پارامترهای رئولوژیکی داشت به طوری که با افزایش درصد صمغ مقادیر G'_{LVE}، G''_{LVE}، مدول در نقطه متقاطع و تنش نقطه جریان افزایش و $\mathrm{Tan}\,\delta_{LVE}$ کاهش پیدا کردند. طبق آزمون فرکانس متغیّر، افزودن آگار به طور معنی داری مقادیر k' و k''را افزایش داد به طوری که مقادیر آنها به ترتیب از ۵۳۱۱/۸ و ۹۳۹/۹ پاسکال در نمونه شاهد تا ۲۵۰۸۰/۶ و ۳۵۷۴/۹ در نمونه حاوی ۰/۷ درصد آگار افزایش یافت. همچنین مقادیر پارامترهای قدرت شبکه (۲۵۳۴۴/۳- ۵۳۸۰/۱ پاسکال.ثانیه) گسترش شبکه (۱۵/۵۹-۱۰/۰۵) و انحراف از قانون کوکس-مرز (۲۱۵۰۹/۴۴-۳۴۷۶/۸۰ پاسکال) به طور مستقیم با افزایش درصد صمغ افزایش پیدا کردند. در ژل امولسیون حاوی ۰/۷ درصد آگار، بیشترین مدول تانژانت اولیه و تنش شکست ثبت شد که این نمونه در مقایسه با نمونه شاهد کرنش شکست کمتر و انرژی شکست مشابه‌ای داشت. همچنین، نتایج پژوهش نشان داد که میزان ظرفیت نگه داری آب در غلظت بالای آگار به طور معنی داری کاهش پیدا می‌کند. این نتایج به دانش برهمکنش پروتئین-پلی ساکارید می‌افزاید که می‌تواند در تولید غذاهای کاربردی جدید مفید باشد.

واژه‌های کلیدی: آگار، ژل امولسیون پر شده سرد، پروتئین آب پنیر، خواص شکست، رئولوژی